

## CHEMISTRY

# Transformation of alcohols to esters promoted by hydrogen bonds using oxygen as the oxidant under metal-free conditions

Mingyang Liu<sup>1,2</sup>, Zhanrong Zhang<sup>1\*</sup>, Huizhen Liu<sup>1,2</sup>, Zhenbing Xie<sup>1,2</sup>, Qingqing Mei<sup>1</sup>, Buxing Han<sup>1,2\*</sup>

One-pot oxidative transformation of alcohols into esters is very attractive, but metal-based catalysts are used in the reported routes. We discovered that the basic ionic liquid 1-ethyl-3-methylimidazolium acetate ([EMIM] OAc) could effectively catalyze this kind of reaction using O<sub>2</sub> as an oxidant without any other catalysts or additives. The oxidative self-esterification of benzylic alcohols or aliphatic alcohols and cross-esterification between benzylic alcohols and aliphatic alcohols could all be achieved with high yields. Detailed study revealed that the cation with acidic proton and basic acetate anion could simultaneously form multiple hydrogen bonds with the hydroxyl groups of the alcohols, which catalyzed the reaction very effectively. As far as we know, this is the first work to carry out this kind of reaction under metal-free conditions.

## INTRODUCTION

Esterification represents one of the most essential reactions in both organic synthesis and the chemical industry. Esters are used as important building blocks for the synthesis of bulk and commodity chemicals having wide applications in pharmaceuticals, polymers, solvents, fragrances, etc. (1–3). In practice, esters are generally synthesized via multistep processes involving the reaction between alcohols and acids or activated acid derivatives (for example, acid chlorides or anhydrides) (1). Although well-established, these processes are becoming increasingly impractical due to the need for handling of corrosive acids and/or their derivatives and generation of large amounts of undesired byproducts. Hence, production of esters in a simple, effective, and economic manner is highly desirable from both scientific and industrial viewpoints.

The direct transformation of alcohols into esters is receiving increasing attention and can avoid the use of hazardous acids and their derivatives and eliminate the generation of undesirable products (for example, aldehydes and acids), leading to significantly improved overall reaction efficiency (4–11). Direct transformation of alcohols into esters can be achieved over catalysts based on metals such as Ru (4, 5, 12), Pd (6, 13), Au (14), Ir (15), or using toxic oxidants such as iodide, bromide, etc. (16). Most of these catalysts are homogeneous and involve noble metals. In recent years, it was reported that direct oxidative esterification of alcohols could also be achieved using cobalt-based (Co and/or Co<sub>3</sub>O<sub>4</sub>) heterogeneous catalysts (7, 8, 11, 17, 18). Given the fact that the catalysts reported so far are generally associated with precious metals and/or tedious procedures for synthesis of effective catalysts, there is a strong need to explore simple, effective, and metal-free alternatives for this class of important reactions. To this end, the development of metal-free catalytic systems using molecular oxygen as a cost-effective oxidant is very attractive but is challenging (19).

Ionic liquids (ILs) are an important class of environmentally benign solvents that have attracted significant attention due to their unique and

attractive properties (20–26), in particular, their negligible vapor pressure, nonflammability, high solubility of gases and substrates, tunable properties by changing anions and/or cations, and ease of recycling. These characteristics make them excellent substitutes for volatile organic compounds in chemical reactions. Among many types of ILs, imidazolium-based basic ILs such as imidazolium-based acetates have shown some specific properties in biomass dissolution, catalytic chemistry, and CO<sub>2</sub>/SO<sub>2</sub> absorption (25, 27–31).

## RESULTS

## Oxidative self-esterification and cross-esterification of benzylic alcohols or aliphatic alcohols

Here, for the first time, we report the application of ILs as both the catalyst and solvent for one-pot conversion of alcohols into their corresponding esters using O<sub>2</sub> as an oxidant under metal-free conditions. Structures of the ILs we used are presented in the Supplementary Materials (fig. S1). It was found that the basic IL 1-ethyl-3-methylimidazolium acetate ([EMIM] OAc) (Table 1, entry 1) showed excellent catalytic performance without any additives, affording benzyl benzoate with yields up to 94%. To investigate the effect of the anion on the reaction, we subsequently conducted the reaction using other imidazolium-based ILs with different anions, including [EMIM] trifluorosulfonate (TFA), [EMIM] HSO<sub>4</sub>, [EMIM] BF<sub>4</sub>, and [EMIM] N(CN)<sub>2</sub>. It was found that these imidazolium-based ILs did not catalyze the reaction, indicating the significant role of the acetate anion for this transformation (Table 1, entries 2 to 5). On the other hand, the [EMIM] cation was crucial for self-esterification of benzyl alcohol because benzyl benzoate could not be generated using 1-octyl-3-methylimidazolium acetate [(OMIM) OAc] or [N<sub>4,4,4,4</sub>] OAc (Table 1, entries 6 and 7). We also prepared NH<sub>4</sub>Ac in a dimethyl sulfoxide (DMSO) solution and found that the mixture was not active for the reaction (Table 1, entry 8). We can deduce from these results that the basic IL composed of [EMIM] cation and OAc<sup>−</sup> anion ([EMIM] OAc) was an excellent catalyst for the reaction, indicating a synergistic and/or cooperative effect between the cation and anion.

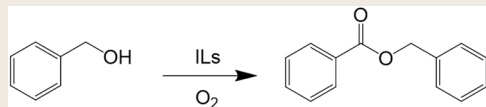
The versatility of [EMIM] OAc was studied using various substituted benzylic alcohols (Table 2) under metal-free conditions. Methyl-substituted benzyl alcohol (that is, 4-methylbenzyl alcohol) could be

Copyright © 2018  
The Authors, some  
rights reserved;  
exclusive licensee  
American Association  
for the Advancement  
of Science. No claim to  
original U.S. Government  
Works. Distributed  
under a Creative  
Commons Attribution  
NonCommercial  
License 4.0 (CC BY-NC).

<sup>1</sup>Beijing National Laboratory for Molecular Sciences, Key Laboratory of Colloid and Interface and Thermodynamics, Institute of Chemistry, Chinese Academy of Sciences, Beijing 100190, P. R. China. <sup>2</sup>University of Chinese Academy of Sciences, Beijing 100049, P. R. China.

\*Corresponding author. Email: hanbx@iccas.ac.cn (B.H.); zhangzhanrong@iccas.ac.cn (Z.Z.)

**Table 1. Self-esterification of benzyl alcohol to benzyl benzoate in various ILs.** Reaction conditions: Benzyl alcohol (2 mmol), 1 MPa O<sub>2</sub>, 2 g of ILs (12 hours, 80°C). Yields were determined using gas chromatography (GC).



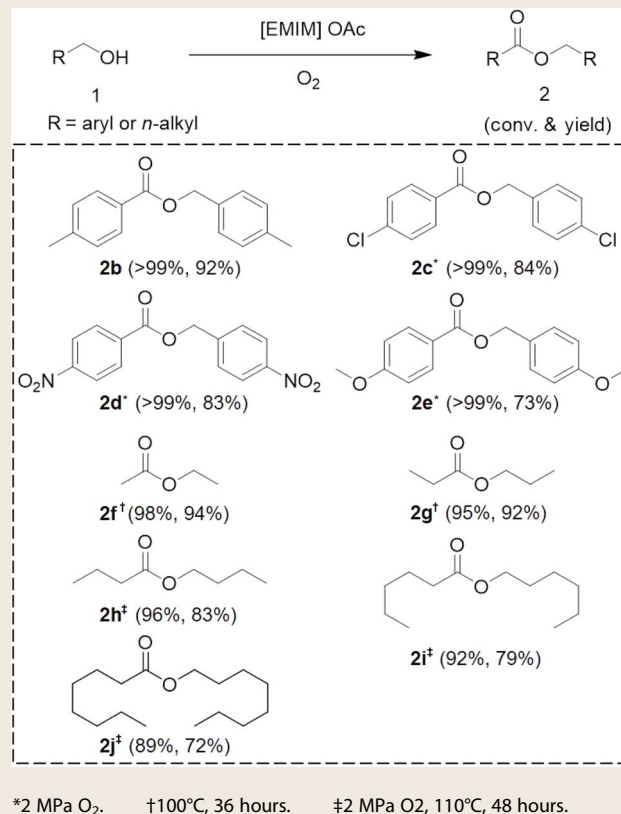
Entry	ILs	Conversion (%)	Yield (%)
1	[EMIM] OAc	>99	94
2	[EMIM] TFA	10	0
3	[EMIM] HSO <sub>4</sub>	16	0
4	[EMIM] BF <sub>4</sub>	3	0
5	[EMIM] N(CN) <sub>2</sub>	<1	0
6	[OMIM] OAc	<1	0
7*	[N <sub>4,4,4,4</sub> ] OAc	26	0
8†	NH <sub>4</sub> Ac/DMSO	5	0

\*Benzyl alcohol (2 mmol), 1 MPa O<sub>2</sub>, 2 g of ILs, 4 hours, 110°C. †Benzyl alcohol (2 mmol), 2 MPa O<sub>2</sub>, 0.4 g of NH<sub>4</sub>Ac, 2 g of DMSO, 12 hours, 80°C.

effectively converted to its corresponding self-esterification product, 4-methylbenzyl 4-methylbenzoate (2b), with an excellent yield of up to 92%. The effect of the electronegativity of the substituent group was studied using substrates with electron-withdrawing groups (Cl and NO<sub>2</sub>), and the yields of corresponding esters for these two substrates were 84 and 83%, respectively (2c and 2d). In the presence of an electron-donating group (OCH<sub>3</sub>), the yield of methoxy-substituted benzyl alcohol-derived ester was 73% (2e), indicating that the presence of an electron-donating substitute group suppresses the activities of benzylic alcohols. In contrast, electron-donating group makes the benzyl protons more electron-rich. Hence, the β-hydride can be easily removed under oxidative conditions, resulting in the generation of more aldehydes (13). Notably, the oxidative self-esterification reaction of benzyl alcohol could also be performed on a multigram scale (200 mmol, 21.6 g) with longer reaction time leading to similar yield of benzyl benzoate (88%; table S1, entry 17).

Aliphatic alcohols are less reactive than benzylic alcohols. Here, aliphatic alcohols with varying chain lengths could also be effectively converted into their corresponding self-esterification esters in [EMIM] OAc under suitable conditions. In general, good yields of corresponding aliphatic esters were achieved from aliphatic alcohols including ethanol, propanol, butanol, hexanol, and octanol. For instance, the direct oxidative esterification of ethanol at 100°C afforded ethyl acetate with a yield of up to 94% (2f). Notably, with the increase of carbon-chain length of the aliphatic alcohol, the yields of corresponding esters decreased, and slightly higher reaction temperature was required. The decrease in yields of esters is attributed to the generation of corresponding acids or aldehydes from the starting aliphatic alcohols. As illustrated in the time course of oxidative esterification of propanol (fig. S2), propanol gradually transformed into propyl propionate, the yield of which reached 92% after 36 hours, together with small amounts of propionic acid (yield of 3%) and propaldehyde (yield

**Table 2. Self-esterification of aryl- and alkyl- Alcohols in [EMIM] OAc.** Reaction conditions: benzyl alcohol (2 mmol), 1 MPa O<sub>2</sub>, 2 g of [EMIM] OAc, 12 hours, 80°C. Yields were determined using GC.



of 5%). Prolonging the reaction time to 48 hours, propaldehyde was fully converted into propionic acid and the yield of propyl propionate remains constant.

Cross-esterification of benzylic and aliphatic alcohols in [EMIM] OAc was also studied, and high yields could be obtained (Table 3). In the presence of excess ethanol, benzyl alcohol was oxidatively esterified to afford ethyl benzoate (3a) with excellent yields of up to 94%. Moreover, methyl-, chloro-, nitro-, and methoxy- substituted benzylic alcohols could be selectively converted to their corresponding ethyl esters with high yields (3b to 3e). The high selectivity for the desired products was primarily attributed to higher activities of benzylic alcohols than that of aliphatic alcohols. Furthermore, the cross-esterification between benzyl alcohol and other long-chain aliphatic alcohols (*n*-butanol, *n*-hexanol, and *n*-octanol) was also achieved. In the presence of excessive amounts of aliphatic alcohol, the yields of targeted ester products were produced up to 87% (3f to 3h). When two different benzylic alcohols were used as substrates, a mixture including their self- and cross-esterification products was generated because of their similar activities (table S1, entry 18).

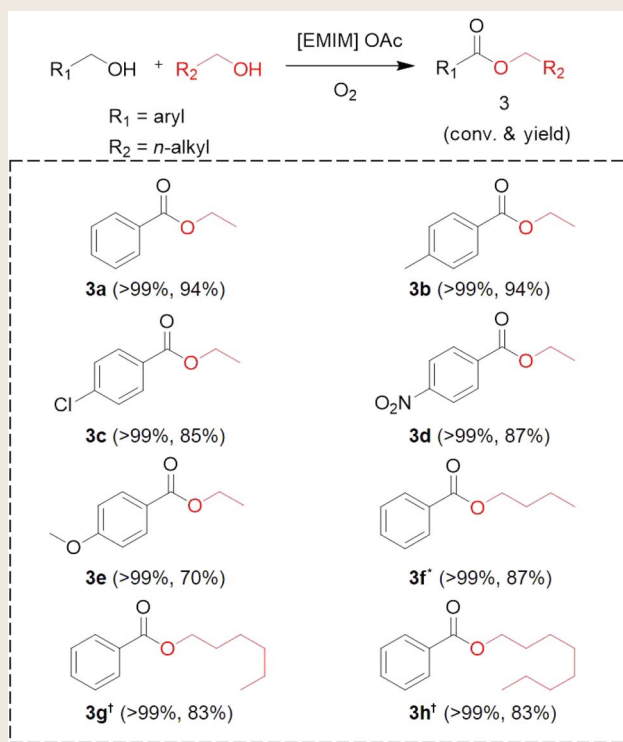
All the experimental results described above demonstrate the wide applicability of [EMIM] OAc. In addition, the basic IL was stable under the reaction conditions and could be easily recycled and reused at least five times without loss of activity (fig. S6).

## DISCUSSION

## Mechanism study

The mechanism for metal-complex-catalyzed oxidative esterification of alcohols to their corresponding esters has been studied (13, 32, 33). Here, we found that the reaction was not affected by the addition of

**Table 3. Cross-esterification of benzylic alcohols and aliphatic alcohols in [EMIM] OAc.** Reaction conditions: Benzyl alcohol (2 mmol), aliphatic alcohol (8 mmol), 2 MPa O<sub>2</sub>, 2 g of [EMIM] OAc, 12 hours, 80°C.



\*90°C, 24 hours. †100°C, 24 hours.

typical radical scavengers such as 2,2,6,6-tetramethylpiperidine-1-oxyl (TEMPO) or butylated hydroxytoluene [2,6-di-*tert*-butyl-4-methylphenol (BHT)] into the reaction (table S1, entries 9 and 10) (34). Hence, this reaction did not proceed via the radical reaction pathway. It is well documented in the literature that 1,3-dialkylimidazolium ILs tend to reactively transform to N-heterocyclic carbenes (NHCs) and weak equilibrium of these ILs, and carbene species exists without an external base or solvent (fig. S7) (30, 35–37). On the basis of the experimental results and the knowledge in literature, we speculate a plausible reaction pathway, as schematically illustrated in Fig. 1.

The hydroxyl group of the alcohol substrate was activated by forming hydrogen bonds with both the [EMIM] cation and acetate anion, affording alcohol-IL complexes (denoted as “a” in Fig. 1). In the presence of O<sub>2</sub>, β-hydride elimination of complex a occurs, leading to the formation of water and corresponding aldehyde b. Because of the equilibrium presence of carbene species in [EMIM] OAc (scheme S1), the carbene attacks the aldehyde b and generates an intermediate complex c, which has a hydroxyl group. This O–H group could form hydrogen bonds with the [EMIM] cation and acetate anion to afford complex d. Subsequently, the complex d transforms to a ketonic intermediate e in O<sub>2</sub>. Then, desired ester products and carbene are released via a substitution reaction between intermediate e and alcohol substrate. The proposed mechanism was further confirmed using isotope labeling experiments with <sup>18</sup>O-enriched benzyl alcohol; for details and discussions, please refer to figs. S9 and S10.

As mentioned, during the oxidative esterification of propanol in [EMIM] OAc, a small amount of propaldehyde (yield of ca. 5%) was detected by GC and its yield did not increase obviously with the reaction time over 36 hours. Thereafter, propaldehyde was converted to propionic acid when reaction time was prolonged to 48 hours (fig. S2). Hence, aldehyde could be possibly an active intermediate. It is noteworthy that for the reactions of benzylic alcohols such as benzyl alcohol, benzaldehyde was not detected by GC. This is probably attributed to their relatively higher electrophilicity in comparison to aliphatic alcohols such as propaldehyde, which renders them highly active in the following reactions with carbene in [EMIM] OAc. However, detailed <sup>1</sup>H NMR characterization verifies the interaction between benzaldehyde and [EMIM] OAc and the existence of aldehyde intermediate (that is, benzaldehyde) during oxidative esterification of

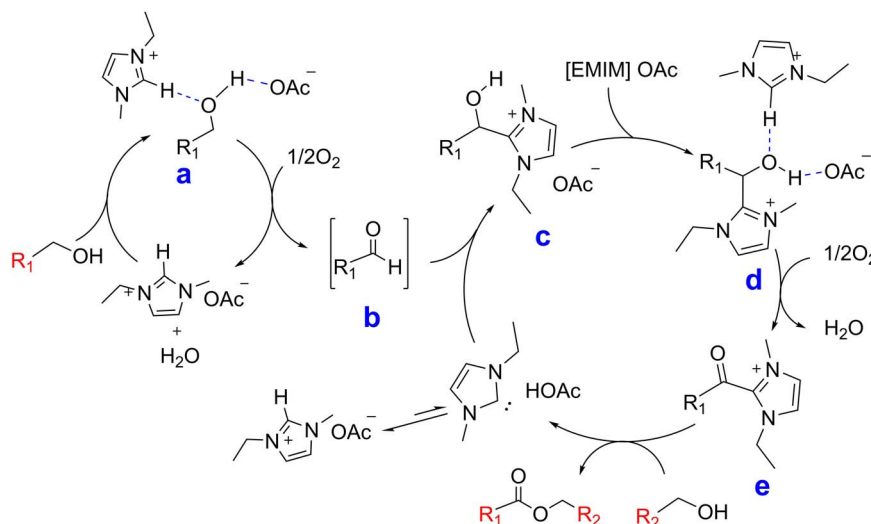


**Fig. 1. Plausible pathway for the oxidative self- or cross-esterification reaction.**

benzyl alcohol (for detailed spectra and discussions, please refer to figs. S3 to S5). As an effort to further verify the presence of active aldehyde **b**, we used identical amounts of benzyl alcohol and benzaldehyde as starting materials; benzyl benzoate was generated stoichiometrically in 3 hours (table S1, entry 13; yield, >99%).

We have also studied the crucial role of NHC for the reaction. As the increasing of side alkyl chain length leads to decreased electronegativity of the imidazolium ring and decreased stability of NHC, the oxidative self-esterification of benzyl alcohol could not be catalyzed by [OMIM] OAc (Table 1, entry 6; and table S1, entry 12). In addition, we investigated the effects of pure NHC on the oxidative esterification reaction. It was found that NHC could induce the esterification of the corresponding aldehyde (that is, benzaldehyde) easily, but not for the alcohol substrate (that is, benzyl alcohol), as highlighted in fig. S8. This effect supports our proposed mechanism that NHC directly attacks the aldehyde intermediate to induce the subsequent oxidative esterification reaction. Similar results on the role of NHC have been previously observed by Sarkar *et al.* (36). It is known that 1,8-diazabicyclo [5.4.0]-7-undecene (DBU) is a strong base with stronger steric hindrance and could potentially promote the formation of NHC (36). However, we found that the addition of DBU into [EMIM] OAc did not promote the oxidative esterification significantly (table S1, entries 5 to 8). On the other hand, water molecules were released during the reaction, resulting in slightly increased moisture content and decreased pH (fig. S18). The decrease of alkalinity could suppress the formation of NHC in [EMIM] OAc. To study this effect, we added additional water into [EMIM] OAc and found that the oxidative esterification reaction of benzyl alcohol was not affected by the addition of small amounts of water (fig. S19). Together, the weak equilibrium between basic IL and NHC is crucial to catalyze the reaction, as NHC could effectively attack the aldehyde intermediate. However, for the [EMIM] OAc promoted oxidative esterification reactions described herein, the variation of amount of NHC does not affect the process of the oxidative esterification reaction. Hence, the NHC-induced oxidation reaction does not represent the rate-determining step.

We propose that the oxidative esterification of alcohols in [EMIM] OAc primarily comprises two steps (Fig. 1). The primary first step is the activation of alcohol O–H group followed by the generation of aldehyde **b**. The second step is the conversion of aldehyde intermediate catalyzed by NHC, which originated from the basic IL. Hence, the first step is of crucial importance to induce the reaction and represents the rate-determining step. Simultaneous formation of multiple hydrogen bonds between [EMIM] cation, acetate anion, and the O and H in the OH group of the alcohols is crucial for activating the alcohol substrates and initiating the esterification reaction. The synergistic effect between the [EMIM] cation and the acetate anion to activate the alcohol O–H group was studied in-depth using a variety of analytical techniques.

Figure 2A illustrates the  $^1\text{H}$  NMR spectra of [EMIM] OAc and the mixtures of benzyl alcohol and [EMIM] OAc with various molar ratios. The resonance band centered at 4.63 parts per million (ppm) in the  $^1\text{H}$  NMR spectrum of benzyl alcohol was assigned to its hydroxyl proton. With continuously increasing [EMIM] OAc content, this resonance band further shifts to 7.76 ppm (molar ratio of 1:5). The downfield shift of the hydroxyl resonance band is mainly ascribed to the formation of hydrogen bonding between hydroxyl protons and the acetate anions (38). Moreover, this resonance band becomes broader, and its full width at half maximum (FWHM) values increased with the increase of [EMIM] OAc content (table S2). These effects result from and reflect the coordination between the hydroxyl

oxygen atoms of benzyl alcohol and the most acidic 2-H protons of [EMIM] OAc (38). Hence, with the synergistic and/or cooperative effect of the cation and anion of [EMIM] OAc, the hydroxyl groups of alcohol substrates were activated, and alcohols were oxidized to afford aldehyde **b** under mild conditions, which initiates the esterification reaction.

For comparison, the interaction between benzyl alcohol and other inactive ILs including [BMIM] TFA and [EMIM]  $\text{BF}_4$  was investigated (Fig. 2, B and C). The hydroxyl resonance band also became broader, indicating the interaction between hydroxyl oxygen atoms of benzyl alcohol and the 2-H protons of imidazolium cation. However, the downfield shift of this resonance band was not observed in either case. These results demonstrate the importance of the synergistic interaction between cation, anion, and alcohol substrates for activating alcohols and for initiating the esterification reaction. The presence of two kinds of hydrogen bonds (that is, hydrogen bonding between hydroxyl groups and [EMIM] and that between hydroxyl groups and acetate anion) can effectively and simultaneously activate the hydroxyl groups of alcohols, thus promoting the oxidative esterification reaction. Furthermore, the specific interaction between [EMIM] OAc and alcohol was verified using Fourier transform infrared spectroscopy (FTIR) (fig. S15 and table S5) and  $^1\text{H}$  diffusion-ordered spectroscopy (DOSY) (fig. S16 and table S6) characterizations.

Since the intensity of the selective  $^1\text{H}$  nuclear Overhauser effects (NOEs) signal is proportional to the ratio of internuclear distance, the nano-environment for this synergistic interaction can be obtained from the integral areas of protons (39). Figure 3 shows the one-dimensional (1D)-selective  $^1\text{H}$  NOE and  $^1\text{H}$  NMR spectra of the mixture of benzyl alcohol and [EMIM] OAc with a molar ratio of 10:1. Initially, we selectively irradiated the hydroxyl resonance [ca. 5.57 ppm], and NOE signals of all other protons were detected (Fig. 3, line 1) in comparison with the  $^1\text{H}$  NMR spectrum (Fig. 3, line 3). This effect implies that the sterical distance between [EMIM] OAc and benzyl alcohol was reduced due to intermolecular interactions. The integral areas of resonance attributed to 5, 6-protons (5.81 and 5.88 ppm) were only around 0.01%, which are much less than that of resonance assigned to the 2-protons of the imidazolium ring (0.48% at about 7.48 ppm), owing to the anisotropy of the imidazolium ring in the mixture. The anisotropy further proves that the hydroxyl group of the alcohol was located near the 2-proton side of the [EMIM] cation, which is consistent with our discussions above. Furthermore, when we selectively irradiated the methyl protons of the acetate anion, the only one positive NOE signal attributed to the hydroxyl group of benzyl alcohol (Fig. 3, line 2) indicated that the methyl group of acetate anion was close to the hydroxyl groups. Hence, the hydroxyl groups of alcohol locate in the middle of the [EMIM] cation and acetate anion and interact simultaneously with the 2-H of [EMIM] cation and acetate anion via hydrogen bonding. The results also support the argument that the cation and anion promote the reaction synergistically.

## CONCLUSION

In summary, the basic IL [EMIM] OAc can catalyze the one-pot oxidative esterification of various alcohols using  $\text{O}_2$  as an oxidant. Not only self-esterification of various benzylic alcohols or aliphatic alcohols but also cross-esterification between them can be achieved directly under mild conditions, affording corresponding ester products with high yields. In the IL-catalyzed reactions, the acidic proton of the [EMIM] cation and the acetate anion can promote the reaction synergistically by

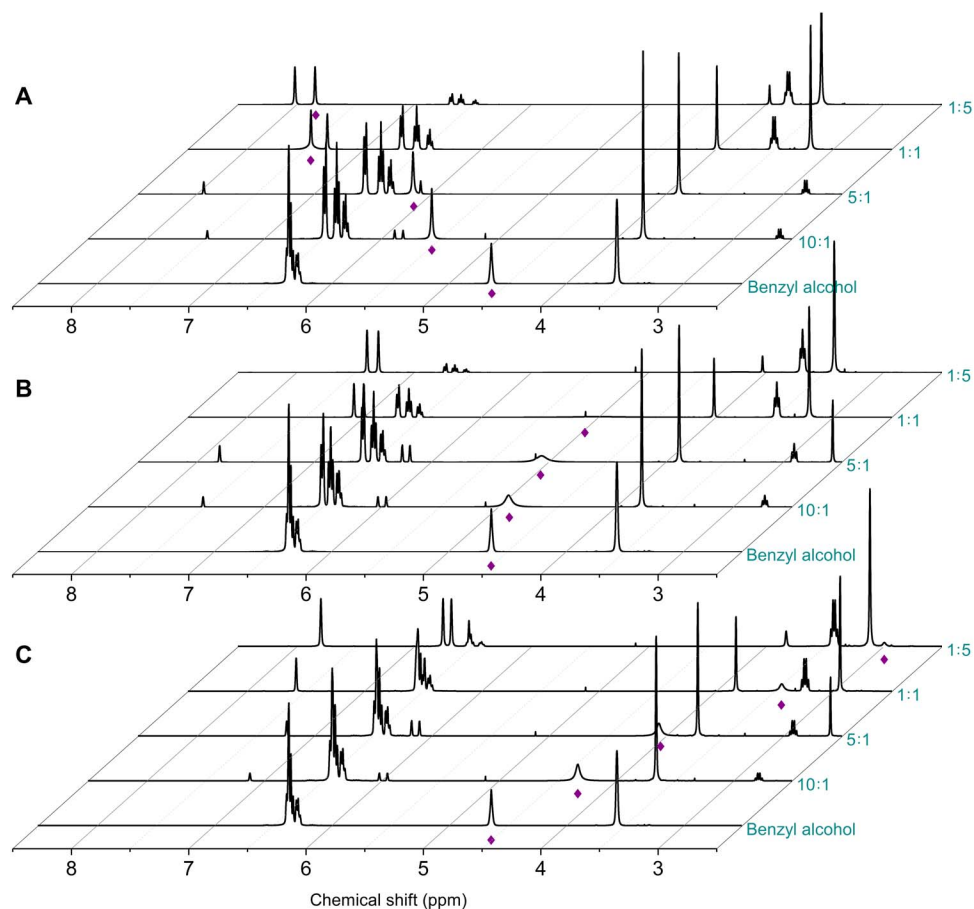


**Fig. 2. The synergistic and/or cooperative effect of the cation and anion of [EMIM] OAc detected by  $^1\text{H}$  NMR spectra.** (A)  $^1\text{H}$  nuclear magnetic resonance (NMR) spectra of benzyl alcohol and its mixtures with [EMIM] OAc with various molar ratios (molar ratio of benzyl alcohol to [EMIM] OAc = 10:1, 5:1, 1:1, and 1:5). (B)  $^1\text{H}$  NMR spectra of benzyl alcohol and its mixtures with [EMIM] TFA. (C)  $^1\text{H}$  NMR spectra of benzyl alcohol and its mixtures with [EMIM]  $\text{BF}_4$ . For recording the spectra, DMSO was used as internal standard. The resonance band of hydroxyl protons is labeled by asterisk. Details are in figs. S4 to S7 and table S2 to S4.

forming hydrogen bonds with the O and H in the OH group of the alcohols, which plays key role for initiating and accelerating the reactions. This work opens the way for carrying out this kind of reactions under metal-free conditions, and the reactions proceed smoothly without any additives. We believe that this simple, efficient, and metal-free route has great potential for application.

## MATERIALS AND METHODS

### Chemicals

DMSO- $d_6$  and substrates including ethanol (99%), propan-1-ol (99%), butan-1-ol (98%), hexan-1-ol (99%), octan-1-ol (99%), benzyl alcohol (99.5%), 4-methylbenzyl alcohol (99%), (4-chlorophenyl)methanol (99.5%), (4-methoxyphenyl)methanol (99.5%), and 4-(hydroxymethyl)phenyl nitrate (99%) were purchased from Acros Organics. Solvents including toluene, diethyl ether, and acetone were purchased from Beijing Chemical Company. DBU, benzylbromide, diphenyl ketone, trioxymethylene, TEMPO, and BHT were purchased from Sigma-Aldrich.  $\text{H}_2^{18}\text{O}$  [97 atomic % (at %)  $^{18}\text{O}$ ] was purchased from InnoChem. All the IL, including [EMIM] OAc, [OMIM] OAc, [EMIM]  $\text{HSO}_4$ ,  $[\text{N}_{4,4,4,4}]$  OAc, [BMIM] TFA, [EMIM]  $\text{BF}_4$ , and [EMIM]  $\text{N}(\text{CN})_2$ , were purchased from the Center for Green Chemistry and Catalysis, Lanzhou Institute of Chem-

ical Physics, Chinese Academy of Sciences. All ILs were dried in a vacuum at  $80^\circ\text{C}$  for 24 hours to remove water or other impurities before use (fig. S17).

### Oxidative esterification of alcohols

Typically, 2 mmol alcohol and 2 g of IL were added into a Teflon-lined stainless-steel reactor. The air in the reactor was replaced by  $\text{O}_2$ , and then more  $\text{O}_2$  was charged to reach the desired pressure. After reaction, the reactor was cooled in an ice-water bath. Products were isolated from the reaction mixture by extracting with toluene three times (for [OMIM] OAc, cyclohexane was used for extraction). Diphenyl ketone, *n*-hexadecane, *n*-dodecane, or *n*-octane was added as an internal standard (according to the boiling point of the corresponding ester products). The qualitative analysis of products was conducted using a GC-mass spectrometer (Agilent 5975C-7890A) and by comparing with authentic samples. The conversion and yields of corresponding esters were quantitatively analyzed by GC (Agilent 6820, equipped with a hydrogen flame-ionization detector, full electric pneumatic control,  $280^\circ\text{C}$ ) based on internal standard curves and areas of integrated peak areas according to the GC traces. To study the reusability, the IL was dried under a vacuum at  $50^\circ\text{C}$  for 24 hours after the extraction process and was then used directly for the next run.

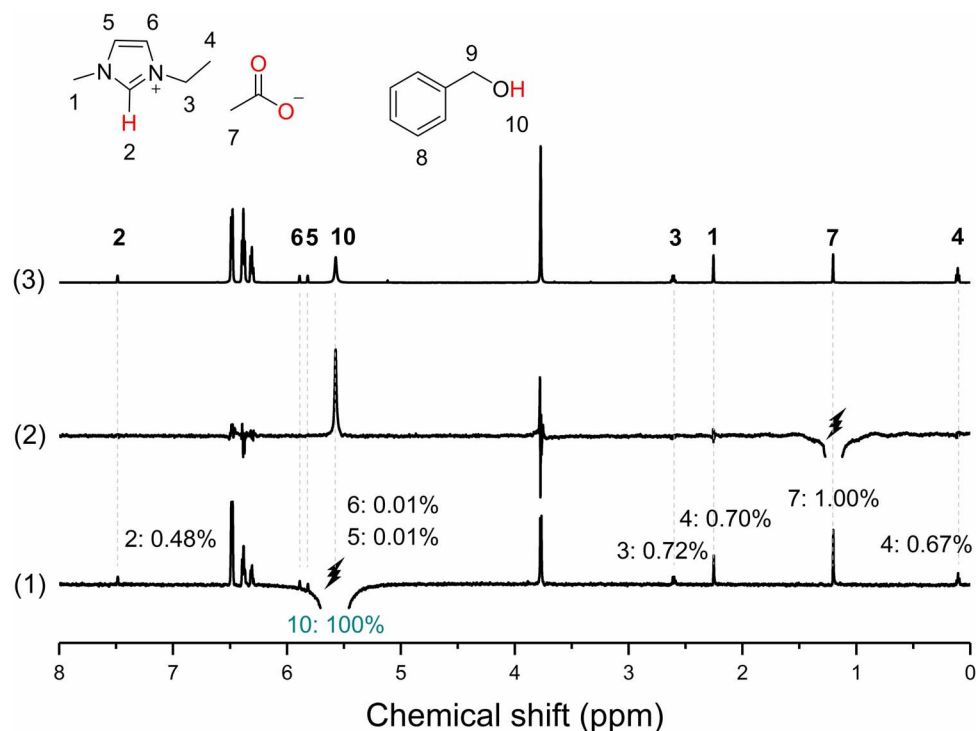


**Fig. 3.** 1D-selective  $^1\text{H}$  NOE and  $^1\text{H}$  NMR spectra of the mixture of benzyl alcohol and [EMIM] OAc. (1) the hydroxyl resonance at 5.57 ppm was selectively irradiated. The integral of the irradiated (negative, peak 10) peak was assigned a value of 100%. The absolute values of other NOE intensities were measured relative to peak 10. (2) The methyl resonance of acetate at 1.20 ppm was selectively irradiated. (3) Normal  $^1\text{H}$  NMR spectrum. The molar ratio of benzyl alcohol to [EMIM] OAc in the mixture was 10:1. *s*-Trioxane was used as an internal standard at 5.11 ppm.

The conversion and yield of the reactions were calculated on the basis of the following equations

$$\text{Conversion} = \left( 1 - \frac{\text{Moles of alcohol remaining}}{\text{Moles of alcohol loaded}} \right) \times 100\%$$

For the yields of self-esterification reactions

$$\text{Yield of product} = \left( \frac{\text{Moles of product} \times 2}{\text{Moles of alcohol loaded}} \right) \times 100\%$$

For the yields of cross-esterification reactions

$$\text{Yield of product} = \left( \frac{\text{Moles of product}}{\text{Moles of alcohol loaded}} \right) \times 100\%$$

### Isotope labeling experiments

$^{18}\text{O}$ -enriched benzyl alcohol was synthesized according to previous work (40). Benzyl bromide (16.7 mmol, 2.00 ml, 1.0 eq), diisopropylethylamine (16.7 mmol, 3.08 ml, 1.0 eq), and heavy water (97 at %  $^{18}\text{O}$ , 16.7 mmol, 300  $\mu\text{l}$ , 1.0 eq) were reacted at 75°C for 24 hours, followed by addition of water (10 ml) and dichloromethane (50 ml). The organic layer was washed with brine for four times. Subsequently, the organic layer was dried with anhydrous  $\text{MgSO}_4$  and evaporated. The resulting product contains two species, namely, benzyl alcohol and dibenzyl ether, and was purified by column chromatography. Yield: 0.76 g  $^{18}\text{O}$ -enriched benzyl alcohol, 87 at %  $^{18}\text{O}$ . The oxidative self-esterification of  $^{18}\text{O}$ -enriched benzyl alcohol and cross-esterification

between  $^{18}\text{O}$ -enriched benzyl alcohol and ethanol was carried out according to the procedure described above.

### NMR measurements

The NMR spectra were recorded on Bruker Avance 400 ( $^1\text{H}$  NMR) and AV-600 (1D-NOESY and 2D-DOSY) equipped with 5-mm pulsed-field gradient (PFG) probes. The spectra were detected at 303 K. To eliminate the effect of solvent, Wilmad coaxial insert NMR tubes were used for  $^1\text{H}$  NMR and 1D-NOESY.  $\text{DMSO-}d_6$  and internal standard were added in the inner tube, and the sample was added in the outer tube.

For  $^1\text{H}$  NMR, the mixtures of benzyl alcohol and [EMIM] OAc with different feed molar ratios were prepared. The mixture (0.3 ml) was added into the outer tube, and the inner tube was inserted. Trioxymethylene was used as internal standard and adjusted at 5.12 ppm if not specified.

For 1D-NOESY, the feed molar ratio of the mixture of benzyl alcohol and [EMIM] OAc was 10:1. The temperature was controlled at 298 K, and no spinning was applied to the NMR tube. The 1D-NOESY was performed at different mixing times from 40 ms to 2 s with a relaxation delay of 2 s and typically 32 transients.

For DOSY, the pure benzyl alcohol and mixture of benzyl alcohol and [EMIM] OAc with a molar ratio of 1:1 was dissolved in  $\text{DMSO-}d_6$ . The concentration of benzyl alcohol was 6  $\text{mg}\cdot\text{ml}^{-1}$ . The temperature was regulated at 299 K, and no spinning was applied to the NMR tube. The DOSY experiments were conducted with a PFG-stimulated echo sequence using bipolar gradients (ledbpgp2s).

### FTIR characterization

The mixtures of benzyl alcohol and [EMIM] OAc with various molar ratios were prepared before analysis. FTIR spectra of the liquid samples

were detected in the transmission mode on a Bruker Vertex 70 infrared spectrometer at a  $1\text{-cm}^{-1}$  resolution. A total of 64 scans were collected for both the reference (pure  $\text{BaF}_2$ ) and the samples.

### Water content and pH measurements

Halogen Moisture Analyzer HC103 (115V) of METTLER TOLEDO was used for water content measurements. Repeatability with 2 g of sample is within 0.1 %. SevenCompact pH meter S210-Bio-Kit of METTLER TOLEDO was used for pH measurements. The pH resolution was 0.01. At specific times, the water content and pH of the reaction medium were measured directly at room temperature after releasing oxygen.

### SUPPLEMENTARY MATERIALS

Supplementary material for this article is available at <http://advances.sciencemag.org/cgi/content/full/4/10/eaas9319/DC1>

Fig. S1. The structures of ILs used in this study.

Fig. S2. Product distributions for the oxidative transformation of propanol to propyl propionate in [EMIM] OAc.

Fig. S3. NMR spectra of benzaldehyde and [EMIM] OAc.

Fig. S4. NMR spectra of the mixture of benzaldehyde and [EMIM] OAc.

Fig. S5.  $^1\text{H}$  NMR spectra of the reaction media of the oxidative esterification reaction of benzyl alcohol (that is, the reaction in Table 1, entry 1) after 3- (yellow) and 12-hour reaction (green), together with that of the mixture of benzaldehyde and [EMIM] OAc (red).

Fig. S6. Recycling of [EMIM] OAc for oxidative esterification of benzyl alcohol and ethanol.

Fig. S7. Possible acid-base equilibrium in [EMIM] OAc.

Fig. S8. Effects of free carbene (products of the reaction between azolium salts A or B and DBU) on the oxidative reactions of benzyl alcohol and benzyl aldehyde.

Fig. S9. Isotope labeling experiments with  $^{18}\text{O}$ -enriched benzyl alcohol.

Fig. S10. Mass spectra of substrates and products for the experiments with  $^{18}\text{O}$ -enriched benzyl alcohol.

Fig. S11.  $^1\text{H}$  NMR spectrum of mixture of benzyl alcohol and [EMIM] OAc (molar ratio of benzyl alcohol to [EMIM] OAc = 1:1).

Fig. S12.  $^1\text{H}$  NMR spectrum of mixture of benzyl alcohol and [EMIM] OAc (molar ratio of benzyl alcohol to [EMIM] OAc = 1:5).

Fig. S13.  $^1\text{H}$  NMR spectra of mixture of benzyl alcohol and [EMIM] TFA (molar ratio of benzyl alcohol to [EMIM] TFA = 1:1).

Fig. S14.  $^1\text{H}$  NMR spectra of mixture of benzyl alcohol and [EMIM] TFA (molar ratio of benzyl alcohol to [EMIM] TFA = 1:5).

Fig. S15. FTIR spectra of benzyl alcohol, [EMIM] OAc, and their mixtures with various molar ratios.

Fig. S16. DOSY NMR spectra.

Fig. S17.  $^1\text{H}$  NMR spectrum of [EMIM] OAc before (above) and after (below) drying in vacuum.

Fig. S18. Variation of moisture content and pH of the reaction media during the oxidative esterification reaction.

Fig. S19. Effects of water content for the oxidative esterification of benzyl alcohol.

Table S1. Self-esterification of benzyl alcohol to benzyl benzoate in various ILs with or without additives.

Table S2. Chemical shifts and FWHM of the hydroxyl group resonance band in  $^1\text{H}$  NMR spectra of the mixtures of benzyl alcohol and [EMIM] OAc with various molar ratios.

Table S3. Chemical shifts and FWHM of the hydroxyl group resonance band in  $^1\text{H}$  NMR spectra of mixture of benzyl alcohol and [BMIM] TFA with various molar ratios.

Table S4. Chemical shifts and FWHM of the hydroxyl group resonance band in  $^1\text{H}$  NMR spectra of mixture of benzyl alcohol and [EMIM]  $\text{BF}_4$  with various molar ratios.

Table S5. Summary of assignments and shifts of frequencies ( $\text{cm}^{-1}$ ) of absorption bands in the FTIR spectra in fig. S15. (v, stretch; s, symmetric; as, antisymmetric).

Table S6. Summary of diffusion coefficients.

### REFERENCES AND NOTES

- J. Otera, J. Nishikido, *Esterification: Methods, Reactions, and Applications* (John Wiley & Sons, 2009).
- A. Das, P. Theato, Activated ester containing polymers: Opportunities and challenges for the design of functional macromolecules. *Chem. Rev.* **116**, 1434–1495 (2016).
- L. Shao, Y.-H. Wang, D.-Y. Zhang, J. Xu, X.-P. Hu, Desilylation-activated propargylic transformation: Enantioselective copper-catalyzed [3+2] cycloaddition of propargylic esters with  $\beta$ -naphthol or phenol derivatives. *Angew. Chem. Int. Ed. Engl.* **55**, 5014–5018 (2016).
- J. Zhang, G. Leitun, Y. Ben-David, D. Milstein, Facile conversion of alcohols into esters and dihydrogen catalyzed by new ruthenium complexes. *J. Am. Chem. Soc.* **127**, 10840–10841 (2005).
- C. Gunanathan, L. J. W. Shimon, D. Milstein, Direct conversion of alcohols to acetals and  $\text{H}_2$  catalyzed by an acridine-based ruthenium pincer complex. *J. Am. Chem. Soc.* **131**, 3146–3147 (2009).
- S. Gowrisankar, H. Neumann, M. Beller, General and selective palladium-catalyzed oxidative esterification of alcohols. *Angew. Chem. Int. Ed.* **50**, 5139–5143 (2011).
- R. V. Jagadeesh, H. Junge, M.-M. Pohl, J. Radnik, A. Brückner, M. Beller, Selective oxidation of alcohols to esters using heterogeneous  $\text{Co}_3\text{O}_4\text{-N@C}$  catalysts under mild conditions. *J. Am. Chem. Soc.* **135**, 10776–10782 (2013).
- Q. Xiao, Z. Liu, A. Bo, S. Zahir, S. Sarina, S. Bottle, J. D. Richey, H. Zhu, Catalytic transformation of aliphatic alcohols to corresponding esters in  $\text{O}_2$  under neutral conditions using visible-light irradiation. *J. Am. Chem. Soc.* **137**, 1956–1966 (2015).
- T. L. Gianetti, S. P. Annen, G. Santiso-Quinones, M. Reiher, M. Driess, H. Grützmaier, Nitrous oxide as a hydrogen acceptor for the dehydrogenative coupling of alcohols. *Angew. Chem. Int. Ed.* **55**, 1854–1858 (2016).
- D. S. Mannel, M. S. Ahmed, T. W. Root, S. S. Stahl, Discovery of multicomponent heterogeneous catalysts via admixture screening: PdBiTe catalysts for aerobic oxidative esterification of primary alcohols. *J. Am. Chem. Soc.* **139**, 1690–1698 (2017).
- H. Su, K.-X. Zhang, B. Zhang, H.-H. Wang, Q.-Y. Yu, X.-H. Li, M. Antonietti, J.-S. Chen, Activating cobalt nanoparticles via the Mott-Schottky effect in nitrogen-rich carbon shells for base-free aerobic oxidation of alcohols to esters. *J. Am. Chem. Soc.* **139**, 811–818 (2017).
- M. Nielsen, H. Junge, A. Kammer, M. Beller, Towards a green process for bulk-scale synthesis of ethyl acetate: Efficient acceptorless dehydrogenation of ethanol. *Angew. Chem. Int. Ed.* **51**, 5711–5713 (2012).
- C. Liu, J. Wang, L. Meng, Y. Deng, Y. Li, A. Lei, Palladium-catalyzed aerobic oxidative direct esterification of alcohols. *Angew. Chem. Int. Ed.* **22**, 5144–5148 (2011).
- H. Miyamura, T. Yasukawa, S. Kobayashi, Aerobic oxidative esterification of alcohols catalyzed by polymer-incarcerated gold nanoclusters under ambient conditions. *Green Chem.* **12**, 776–778 (2010).
- N. Yamamoto, Y. Obora, Y. Ishii, Iridium-catalyzed oxidative methyl esterification of primary alcohols and diols with methanol. *J. Org. Chem.* **76**, 2937–2941 (2011).
- X. Liu, J. Wu, Z. Shang, Efficient dimeric esterification of alcohols with NBS in water using L-proline as catalyst. *Synth. Commun.* **42**, 75–83 (2012).
- R. V. Jagadeesh, T. Stemmler, A.-E. Surkus, M. Bauer, M.-M. Pohl, J. Radnik, K. Junge, H. Junge, A. Brückner, M. Beller, Cobalt-based nanocatalysts for green oxidation and hydrogenation processes. *Nat. Protoc.* **10**, 916–926 (2015).
- W. Zhong, H. Liu, C. Bai, S. Liao, Y. Li, Base-free oxidation of alcohols to esters at room temperature and atmospheric conditions using nanoscale Co-based catalysts. *ACS Catal.* **5**, 1850–1856 (2015).
- K. S. Egorova, V. P. Ananikov, Which metals are green for catalysis? Comparison of the toxicities of Ni, Cu, Fe, Pd, Pt, Rh, and Au salts. *Angew. Chem. Int. Ed.* **55**, 12150–12162 (2016).
- V. I. Părvulescu, C. Hardacre, Catalysis in ionic liquids. *Chem. Rev.* **107**, 2615–2665 (2007).
- J. P. Hallett, T. Welton, Room-temperature ionic liquids: Solvents for synthesis and catalysis. 2. *Chem. Rev.* **111**, 3508–3576 (2011).
- H. Zhao, J. E. Holladay, H. Brown, Z. C. Zhang, Metal chlorides in ionic liquid solvents convert sugars to 5-hydroxymethylfurfural. *Science* **316**, 1597–1600 (2007).
- J. Li, W. Yang, S. Yang, L. Huang, W. Wu, Y. Sun, H. Jiang, Palladium-catalyzed cascade annulation to construct functionalized  $\beta$ - and  $\gamma$ -lactones in ionic liquids. *Angew. Chem. Int. Ed.* **53**, 7219–7222 (2014).
- B. A. Rosen, A. Salehi-Khojin, M. R. Thorson, W. Zhu, D. T. Whipple, P. J. A. Kenis, R. I. Masel, Ionic liquid-mediated selective conversion of  $\text{CO}_2$  to CO at low overpotentials. *Science* **334**, 643–644 (2011).
- Z. Zhang, J. Song, B. Han, Catalytic transformation of lignocellulose into chemicals and fuel products in ionic liquids. *Chem. Rev.* **117**, 6834–6880 (2017).
- C. Dai, J. Zhang, C. Huang, Z. Lei, Ionic liquids in selective oxidation: Catalysts and solvents. *Chem. Rev.* **117**, 6929–6983 (2017).
- Y. Pu, N. Jiang, A. J. Ragauskas, Ionic liquid as a green solvent for lignin. *J. Wood Chem. Technol.* **27**, 23–33 (2007).
- M. B. Shiflett, A. Yokozeki, Chemical absorption of sulfur dioxide in room-temperature ionic liquids. *Ind. Eng. Chem. Res.* **49**, 1370–1377 (2009).
- M. Zavrel, D. Bross, M. Funke, J. Büchs, A. C. Spiess, High-throughput screening for ionic liquids dissolving (ligno-) cellulose. *Bioresour. Technol.* **100**, 2580–2587 (2009).
- G. Gurau, H. Rodríguez, S. P. Kelley, P. Janiczek, R. S. Kalb, R. D. Rogers, Demonstration of chemisorption of carbon dioxide in 1,3-dialkylimidazolium acetate ionic liquids. *Angew. Chem. Int. Ed.* **50**, 12024–12026 (2011).
- C. J. Clarke, W.-C. Tu, O. Levers, A. Bröhl, J. P. Hallett, Green and sustainable solvents in chemical processes. *Chem. Rev.* **118**, 747–800 (2018).
- J. Rabeah, U. Benstrup, R. Stößer, A. Brückner, Selective alcohol oxidation by a copper-TEMPO catalyst: Mechanistic insights by simultaneously coupled operando EPR/UV-vis/ATR-IR spectroscopy. *Angew. Chem. Int. Ed.* **54**, 11791–11794 (2015).
- B. Xu, J.-P. Lumb, B. A. Arndtsen, A TEMPO-free copper-catalyzed aerobic oxidation of alcohols. *Angew. Chem. Int. Ed.* **54**, 4208–4211 (2015).

34. H. Li, Y. Zhao, L. Ma, M. Ma, J. Jiang, X. Wan, Radical-carbene coupling reaction: Mn-catalyzed synthesis of indoles from aromatic amines and diazo compounds. *Chem. Commun.* **53**, 5993–5996 (2017).
35. T.-Y. Jian, L. He, C. Tang, S. Ye, N-Heterocyclic carbene catalysis: Enantioselective formal [2+2] cycloaddition of ketenes and *N*-sulfinylanilines. *Angew. Chem. Int. Ed.* **50**, 9104–9107 (2011).
36. S. De Sarkar, A. Biswas, R. C. Samanta, A. Studer, Catalysis with N-heterocyclic carbenes under oxidative conditions. *Chemistry* **19**, 4664–4678 (2013).
37. M. Fèvre, J. Pinaud, A. Leteneur, Y. Gnanou, J. Vignolle, D. Taton, K. Miqueu, J.-M. Sotiropoulos, Imidazol(in)ium hydrogen carbonates as a genuine source of *N*-heterocyclic carbenes (NHCs): Applications to the facile preparation of NHC metal complexes and to NHC-organocatalyzed molecular and macromolecular syntheses. *J. Am. Chem. Soc.* **134**, 6776–6784 (2012).
38. J. Zhang, H. Zhang, J. Wu, J. Zhang, J. He, J. Xiang, NMR spectroscopic studies of cellobiose solvation in EMIN Ac aimed to understand the dissolution mechanism of cellulose in ionic liquids. *Phys. Chem. Chem. Phys.* **12**, 1941–1947 (2010).
39. B. Vögeli, The nuclear Overhauser effect from a quantitative perspective. *Prog. Nucl. Magn. Reson. Spectrosc.* **78**, 1–46 (2014).
40. A. Hofer, G. S. Cremonnik, A. C. Müller, R. Giamb Bruno, C. Trefzer, G. Superti-Furga, K. L. Bennett, H. J. Jessen, A modular synthesis of modified phosphoanhydrides. *Chemistry* **21**, 10116–10122 (2015).

#### Acknowledgments

**Funding:** This work was supported financially by National Natural Science Foundation of China (21603236, 21733011), National Key Research and Development Program of China (2017YFA0403103), and Chinese Academy of Sciences (QYZDY-SSW-SLH013). **Author contributions** M.L., Z.Z., and B.H. proposed the project and designed and conducted the experiments. M.L., Z.Z., and B.H. discussed and wrote the manuscript. All other authors discussed the work. **Competing interests:** The authors declare that they have no competing interests. **Data and materials availability:** All data needed to evaluate the conclusions in the paper are present in the paper and/or the Supplementary Materials. Additional data related to this paper may be requested from the authors.

Submitted 6 January 2018

Accepted 28 August 2018

Published 5 October 2018

10.1126/sciadv.aas9319

**Citation:** M. Liu, Z. Zhang, H. Liu, Z. Xie, Q. Mei, B. Han, Transformation of alcohols to esters promoted by hydrogen bonds using oxygen as the oxidant under metal-free conditions. *Sci. Adv.* **4**, eaas9319 (2018).



## Transformation of alcohols to esters promoted by hydrogen bonds using oxygen as the oxidant under metal-free conditions

Mingyang Liu, Zhanrong Zhang, Huizhen Liu, Zhenbing Xie, Qingqing Mei and Buxing Han

*Sci Adv* 4 (10), eaas9319.  
DOI: 10.1126/sciadv.aas9319

ARTICLE TOOLS	<a href="http://advances.sciencemag.org/content/4/10/eaas9319">http://advances.sciencemag.org/content/4/10/eaas9319</a>
SUPPLEMENTARY MATERIALS	<a href="http://advances.sciencemag.org/content/suppl/2018/10/01/4.10.eaas9319.DC1">http://advances.sciencemag.org/content/suppl/2018/10/01/4.10.eaas9319.DC1</a>
REFERENCES	This article cites 39 articles, 2 of which you can access for free <a href="http://advances.sciencemag.org/content/4/10/eaas9319#BIBL">http://advances.sciencemag.org/content/4/10/eaas9319#BIBL</a>
PERMISSIONS	<a href="http://www.sciencemag.org/help/reprints-and-permissions">http://www.sciencemag.org/help/reprints-and-permissions</a>

Use of this article is subject to the [Terms of Service](#)

---

*Science Advances* (ISSN 2375-2548) is published by the American Association for the Advancement of Science, 1200 New York Avenue NW, Washington, DC 20005. 2017 © The Authors, some rights reserved; exclusive licensee American Association for the Advancement of Science. No claim to original U.S. Government Works. The title *Science Advances* is a registered trademark of AAAS.